

1 **Multiple T6SSs, mobile auxiliary modules, and effectors revealed in a systematic**
2 **analysis of the *Vibrio parahaemolyticus* pan-genome**

3 Biswanath Jana¹, Kinga Keppel¹, Chaya Mushka Fridman¹, Eran Bosis^{2,#}, & Dor Salomon^{1,#}

4

5 ¹ Department of Clinical Microbiology and Immunology, Sackler Faculty of Medicine, Tel Aviv
6 University, Tel Aviv, Israel

7 ² Department of Biotechnology Engineering, Braude College of Engineering, Karmiel, Israel

8 # Corresponding authors. Tel: +972 3 6408583; E-mail: dorsalomon@mail.tau.ac.il (DS); Tel:
9 +972 4 9901927; E-mail: boasis@braude.ac.il (EB)

10

11 **Running title:** Pan-genome repertoire of *Vibrio parahaemolyticus* T6SS

12 **Key words:** T6SS, antibacterial, competition, secretion, Vibrio

13

14 **Abstract**

15 Type VI secretion systems (T6SSs) play a major role in interbacterial competition and in bacterial
16 interactions with eukaryotic cells. The distribution of T6SSs and the effectors they secrete vary
17 between strains of the same bacterial species. Therefore, a pan-genome investigation is required
18 to better understand the T6SS potential of a bacterial species of interest. Here, we performed a
19 comprehensive, systematic analysis of T6SS gene clusters and auxiliary modules found in the
20 pan-genome of *Vibrio parahaemolyticus*, an emerging pathogen widespread in marine
21 environments. We identified four different T6SS gene clusters within genomes of this species; two
22 systems appear to be ancient and widespread, whereas the other two systems are rare and
23 appear to have been more recently acquired via horizontal gene transfer. In addition, we identified
24 diverse T6SS auxiliary modules containing putative effectors with either known or predicted toxin
25 domains. Many auxiliary modules are possibly horizontally shared between *V. parahaemolyticus*
26 genomes, since they are flanked by DNA mobility genes. We further investigated a DUF4225-
27 containing protein encoded on an Hcp auxiliary module, and we showed that it is an antibacterial
28 T6SS effector that exerts its toxicity in the bacterial periplasm, leading to cell lysis. Computational
29 analyses of DUF4225 revealed a widespread toxin domain associated with various toxin delivery
30 systems. Taken together, our findings reveal a diverse repertoire of T6SSs and auxiliary modules
31 in the *V. parahaemolyticus* pan-genome, as well as novel T6SS effectors and toxin domains that
32 can play a major role in the interactions of this species with other cells.

33

34 **Importance**

35 Gram-negative bacteria employ toxin delivery systems to mediate their interactions with
36 neighboring cells. *Vibrio parahaemolyticus*, an emerging pathogen of humans and marine
37 animals, was shown to deploy antibacterial toxins into competing bacteria via the type VI secretion
38 system (T6SS). Here, we analyzed 1,727 *V. parahaemolyticus* genomes and revealed the pan-
39 genome T6SS repertoire of this species, including the T6SS gene clusters, horizontally shared
40 auxiliary modules, and toxins. We also identified a role for a previously uncharacterized domain,
41 DUF4225, as a widespread antibacterial toxin associated with diverse toxin delivery systems.

42

43 Introduction

44 During competition, bacteria deliver toxic cocktails of effectors using specialized, contact-
45 dependent protein secretion systems (1). Gram-negative bacteria often employ the type VI
46 secretion system (T6SS) to gain a competitive advantage over their rivals (2). This system
47 comprises 13-14 core components, in addition to accessory components that differ between
48 systems and may play different regulatory roles (3–6). The structural and regulatory components
49 of T6SS are encoded within large gene clusters that also often encode effectors; effectors are
50 also encoded within auxiliary modules containing T6SS core components (7–10), or within orphan
51 cassettes (11, 12). The effectors are loaded onto a missile-like structure comprising a tube
52 consisting of stacked rings of Hcp hexamers; the tube is capped by a spike complex composed
53 of a VgrG trimer sharpened by a PAAR repeat-containing protein (hereafter referred to as PAAR)
54 (13). The loaded missile is propelled outside of the cell by a contracting sheath that engulfs it (14);
55 the contraction provides sufficient force to penetrate into a neighboring cell and deploy the
56 effectors (5).

57 Many effector families that contain toxin domains that mediate antibacterial activities have been
58 reported. Effectors often target conserved bacterial components in the cytoplasm or periplasm,
59 such as nucleic acids (nucleases) (7, 15–19), the membrane (phospholipases and pore-forming
60 toxins) (10, 11, 20–22), or the peptidoglycan layer (amidases, glycoside hydrolases, and carboxy-
61 and transpeptidases) (12, 23, 24). Additional activities mediated by T6SS effectors include the
62 following: altering the energy balance by hydrolyzing NAD(P)⁺ (25, 26), ADP-ribosylating the
63 conserved protein FtsZ to inhibit cell division (27), ADP-ribosylating the 23S rRNA to inhibit
64 translation (28), targeting the transamidosome to inhibit protein synthesis (29), deaminating the
65 target cell's DNA (30), and synthesizing the toxic molecule (p)ppApp (31). Antibacterial T6SS
66 effectors are encoded adjacent to cognate immunity proteins that protect against self- or kin-
67 intoxication (2, 32). Several experimental and computational approaches have been used to
68 identify effector and immunity (E/I) pairs (2, 7, 11, 12, 29, 33–36). Nevertheless, because T6SS
69 effectors employ diverse mechanisms for secretion (13, 37–39), and therefore lack a canonical
70 secretion signal, it is estimated that many more effectors still await discovery.

71 *Vibrio parahaemolyticus* is an emerging pathogen that inhabits marine and estuarine
72 environments (40). Previous works revealed that all investigated *V. parahaemolyticus* isolates
73 contain a T6SS on chromosome 2, named T6SS2, whereas pathogenic isolates encode another
74 T6SS on chromosome 1, named T6SS1 (41–43). The presence of additional T6SSs in this
75 species remains to be investigated. T6SS2 was recently shown to mediate antibacterial activities;
76 however, its effector repertoire remains unstudied (11, 44). T6SS1, which has been studied in
77 several isolates (7, 11, 36, 42, 43), also mediates antibacterial activities. Each isolate contains
78 conserved antibacterial E/I pairs, which are encoded by the main T6SS1 gene cluster, as well as
79 “accessory” E/I pairs that differ between isolates and diversify the effector repertoire (36, 45). To
80 date, accessory T6SS1 E/I pairs were found in auxiliary T6SS modules containing a gene
81 encoding VgrG (7), or as orphan operons that often reside next to DNA mobility elements (11, 36,
82 42). Notably, since most vibrios are naturally competent (46, 47), horizontal gene transfer (HGT)
83 may play a role in the acquisition and evolution of the T6SS E/I pair repertoire (48, 49).

84 In this study, we sought to reveal the collective repertoire of T6SS gene clusters and auxiliary
85 modules in *V. parahaemolyticus*, as well as to identify new effectors. By systematically analyzing
86 1,727 *V. parahaemolyticus* genomes, we identified four types of T6SS gene clusters and many
87 distinct, widespread auxiliary modules predicted to encode diverse effectors; the vast majority of
88 the auxiliary modules, as well as two of the T6SS gene clusters, are found next to DNA mobility
89 genes, suggesting that they were acquired via HGT. Intriguingly, most *hcp*-containing auxiliary
90 modules encode a previously undescribed effector with a C-terminal domain of unknown function

91 4225 (DUF4225). We experimentally showed that this effector is toxic upon delivery to the
92 bacterial periplasm, where it leads to cell lysis. We also identified a downstream-encoded cognate
93 immunity protein that antagonizes the effector's toxic effect. Surprisingly, although several strains
94 of marine bacteria were intoxicated by this effector during competition, others, including two *V.*
95 *parahaemolyticus* strains that do not contain homologs of the cognate immunity protein, were
96 resistant to the attack. Further analysis revealed that DUF4225 is a widespread toxin domain that
97 is present in polymorphic toxins associated with several protein secretion systems.

98

99 **Results**

100 **Four T6SS gene clusters are found in the *V. parahaemolyticus* pan-genome**

101 We first set out to identify the T6SS gene clusters found in the *V. parahaemolyticus* pan-genome.
102 To this end, we retrieved the sequences of the conserved T6SS core component, TssB (3), from
103 1,727 available RefSeq *V. parahaemolyticus* genomes ([Supplementary Dataset S1](#)). Analysis
104 of the phylogenetic distribution of TssB revealed four groups ([Fig. 1A](#)) corresponding to four
105 distinct T6SS gene clusters in *V. parahaemolyticus* genomes ([Fig. 1B](#) and [Supplementary](#)
106 [Dataset S2,S3](#)).

107 T6SS1 and T6SS2 were previously investigated and found to mediate interbacterial competition
108 (7, 11, 36, 43, 44). In agreement with previous analyses on smaller genome datasets (7, 11, 43),
109 we identified T6SS2 in nearly all *V. parahaemolyticus* genomes (99%), whereas T6SS1 was
110 identified in 68.3% of the genomes ([Fig. 1b](#), [Fig. 2](#), and [Supplementary Dataset S2,S3](#)). We did
111 not identify known or potential effectors encoded within the T6SS2 gene clusters; however, the
112 T6SS1 clusters contain two antibacterial effectors, corresponding to VP1390 and VP1415 in the
113 type strain RIMD 2210633 (36, 37) ([Table 1](#)). Interestingly, we observed some diversity at the
114 end of T6SS1 gene clusters; we found what appears to be duplications (between one and six
115 copies) of the PAAR-containing specialized effector, corresponding to VP1415 in the type strain
116 RIMD 2210633 (36).

117 Two additional T6SS gene clusters, which we named T6SS3 and T6SS4 ([Fig. 1b](#)), have a limited
118 distribution in *V. parahaemolyticus* genomes (0.8% and 1.8%, respectively) ([Fig. 2](#), and
119 [Supplementary Dataset S2,S3](#)). T6SS3 is similar to the previously reported T6SS3 of *V.*
120 *proteolyticus*, which was suggested to have anti-eukaryotic activity (50). T6SS4 could be further
121 divided into three sub-groups, a-c, with minor differences in gene sequence and content ([Fig. 1b](#)
122 and [Supplementary Dataset S3](#)). We identified potential effectors encoded in both the T6SS3
123 and T6SS4 gene clusters ([Fig. 1b](#) and [Table 1](#)). Notably, T6SS3 and T6SS4, which were not
124 previously described in *V. parahaemolyticus*, are flanked by transposases and other DNA mobility
125 elements ([Fig. 1](#)), suggesting that they have been acquired via HGT. Taken together, these
126 results reveal that the *V. parahaemolyticus* pan-genome contains two widespread T6SSs and two
127 T6SSs with limited distribution.

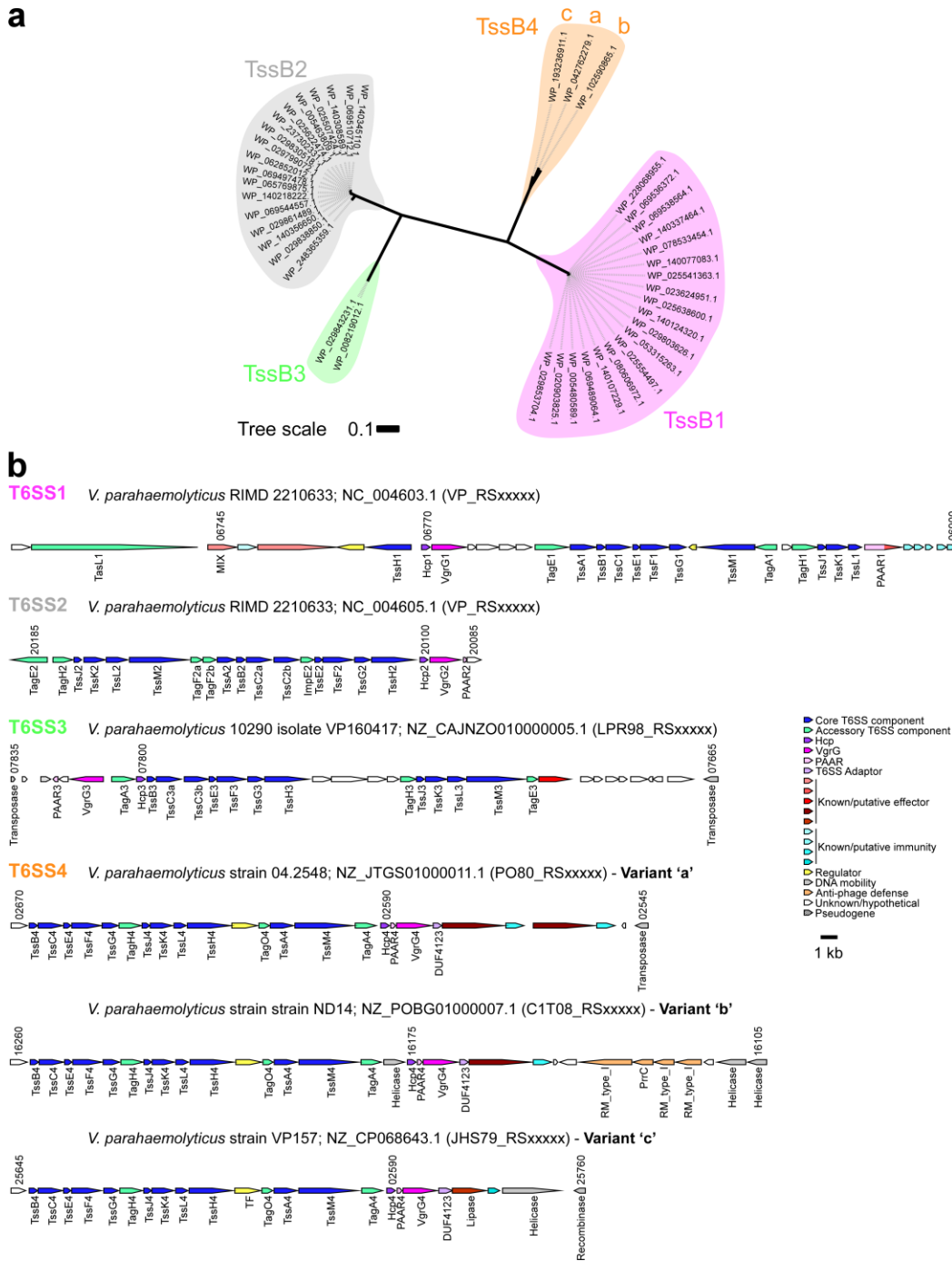


Figure 1. The *V. parahaemolyticus* pan-genome harbors four T6SSs. (a) Phylogenetic distribution of the T6SS core component TssB encoded within *V. parahaemolyticus* genomes. The evolutionary history was inferred using the neighbor-joining method. The phylogenetic tree was drawn to scale, with branch lengths in the same units as those of the evolutionary distances used to infer the phylogenetic tree. The evolutionary distances were computed using the Poisson correction method; they are in the units of the number of amino acid substitutions per site. (b) Representative T6SS gene clusters found in *V. parahaemolyticus* genomes. The strain names, the GenBank accession numbers, and the locus tag annotation patterns are provided. Genes are denoted by arrows indicating the direction of transcription. Locus tags are denoted above, and the names of encoded proteins or domains are denoted below.

129 Diverse and widespread T6SS auxiliary modules contain effectors

130 Although T6SS effectors are often encoded within the main T6SS gene clusters, auxiliary modules
131 containing at least one secreted T6SS component (i.e., Hcp, VgrG, or PAAR) and downstream-
132 encoded effectors are also common (7–10). Therefore, to identify auxiliary T6SS modules, we
133 searched the *V. parahaemolyticus* pan-genome for Hcp, VgrG, and PAAR encoded outside the
134 four main T6SS gene clusters described above. We found diverse auxiliary module types widely
135 distributed among the different *V. parahaemolyticus* genomes (**Fig. 2, Supplementary Fig. S1,**
136 **and Supplementary Dataset S2,S4**). These modules are predominantly found next to DNA
137 mobility genes, such as integrases, recombinases, transposases, phage proteins, or plasmid
138 mobility elements. Notably, some modules contain more than one secreted T6SS component,
139 and some genomes harbor multiple module types (up to seven modules in one genome).

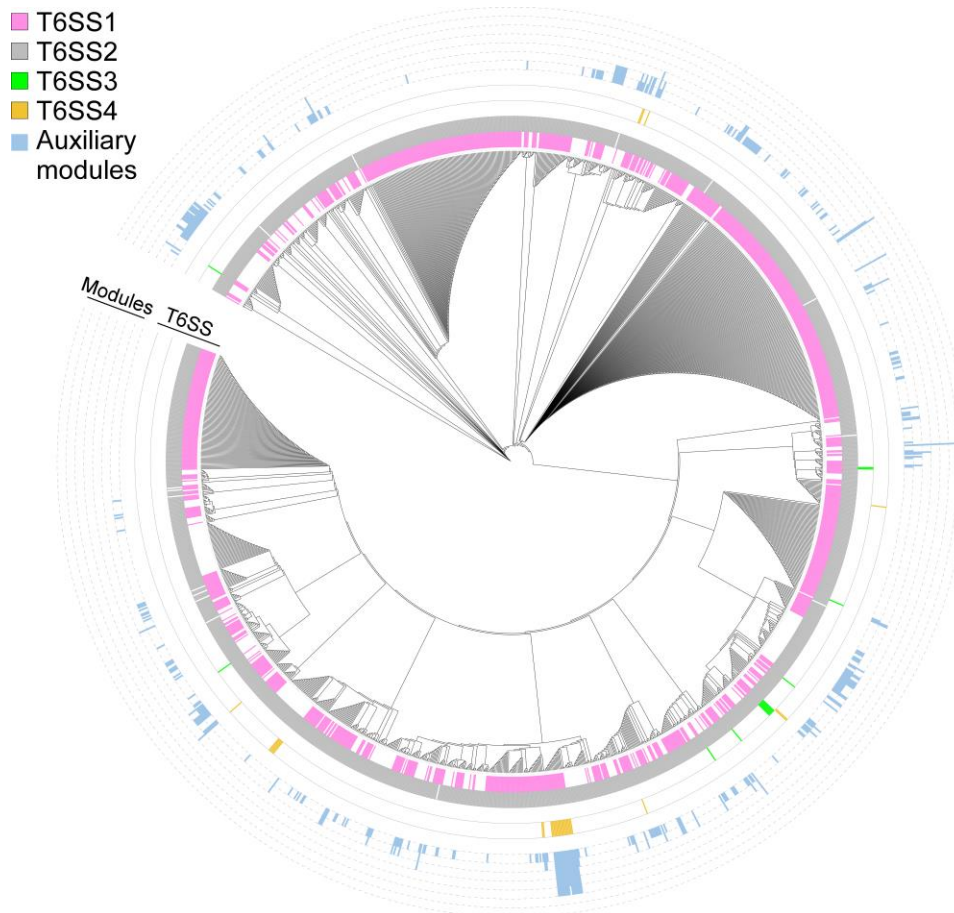


Figure 2. Distribution of T6SS gene clusters and auxiliary modules in *V. parahaemolyticus*. The phylogenetic tree was based on DNA sequences of *rpoB* coding for DNA-directed RNA polymerase subunit beta. The evolutionary history was inferred using the neighbor-joining method. The height of the blue bars denoted the number of T6SS auxiliary modules per genome.

140 PAAR proteins encoded within auxiliary modules are often specialized effectors containing known
141 (e.g., AHH, Ntox15, and NUC nucleases) or predicted C-terminal toxin domains (**Table 1**),
142 followed by a downstream gene that possibly encodes a cognate immunity protein
143 (**Supplementary Fig. S1** and **Supplementary Dataset S4**). Homologous PAAR proteins are also
144 encoded within similar auxiliary module configurations in which the toxin domain is encoded by a
145 separate gene as a possible cargo effector (**Table 1** and **Supplementary Dataset S4**). In

146 contrast, we did not identify auxiliary VgrG proteins containing C-terminal toxin domains; instead,
 147 auxiliary VgrG modules carry cargo effectors, some with known activities (e.g., PoNe DNase,
 148 NucA/B nuclease, and Lip2 lipase). These cargo effectors are mostly encoded downstream of a
 149 gene encoding a T6SS adaptor protein, such as DUF4123, DUF2169, and DUF1795 (39, 51)
 150 (**Supplementary Fig. S1** and **Supplementary Dataset S4**).

151 Hcp-encoding auxiliary modules contain a few, previously uncharacterized, putative cargo
 152 effectors of unknown function (**Table 1**, **Supplementary Fig. S1** and **Supplementary Dataset**
 153 **S4**). Interestingly, in most Hcp-containing auxiliary modules that we found, which are located in
 154 diverse synteny, a DUF4225-containing protein is encoded immediately downstream of *hcp*
 155 (**Supplementary Fig. S2**). Some DUF4225-encoding genes have an adjacent, small gene
 156 encoding a protein predicted to contain transmembrane helices (according to a Phobius server
 157 analysis (52)) (**Supplementary Dataset S4**). Based on these findings, we hypothesized that
 158 these DUF4225-encoding genes and their downstream adjacent genes are antibacterial T6SS E/I
 159 pairs.

160

161 **Table 1. Predicted effectors in *V. parahaemolyticus* T6SS clusters and auxiliary modules.**

Example accession number	Example gene locus	Found in T6SS or module type	Effector type	Predicted toxin domain	Predicted activity	Homologs in other polymorphic toxin classes	Ref.
WP_005480617.1	VP_RS06755 (VP1390)	T6SS1	Cargo	Unknown	Cell lysis	No	(37)
WP_005493834.1	VP_RS06875 (VP1415)	T6SS1, PAAR	Specialized / Cargo	AHH	Nuclease	Yes	(36, 53)
WP_029843206.1	LPR98_RS07710	T6SS3	Cargo	Unknown	Unknown	Yes	
WP_042762256.1	PO80_RS02570	T6SS4a,b	Cargo	Unknown	Unknown	No	
WP_193237005.1	JHS79_RS25745	T6SS4c, Hcp+VgrG	Cargo	Lip2	Lipase	Yes	
WP_065771704.1	AKH09_RS09365	PAAR+VgrG+Hcp	Cargo	Unknown	Unknown	Yes	
WP_238790300.1	K6U37_RS14065	PAAR+VgrG	Cargo	NucA/B	Nuclease	Yes	(53)
WP_020841305.1	H9J98_RS02420	PAAR	Specialized / Cargo	Ntox15	Nuclease	Yes	(15, 53)
WP_083135234.1	GPY55_RS17385	PAAR	Specialized / Cargo	NUC	Nuclease	Yes	(53)
WP_102591288.1	C1T08_RS26340	PAAR	Specialized	Unknown	Unknown	Yes	
WP_102591220.1	C1S85_RS24675	PAAR	Specialized	Tme	Membrane-disrupting	Yes	(11)
WP_102591225.1	C1S85_RS24700	PAAR	Specialized	Unknown	Unknown	Yes	
WP_238789479.1	K6U37_RS04455	PAAR	Specialized (truncated)	Unknown	Unknown	Yes	
WP_129147717.1	EGL73_RS17180	VgrG	Cargo	Unknown	Unknown	No	(54)
WP_029857615.1	B5C30_RS14465	VgrG	Cargo	PoNe	DNase	Yes	(7)
WP_238790289.1	K6U37_RS13990	VgrG	Cargo	Unknown	Unknown	Yes	(45)
WP_086585359.1	JHS88_RS14235	Hcp	Cargo	DUF4225	Cell lysis	Yes	This work
WP_195433156.1	K6U37_RS12660	Hcp	Cargo	Unknown	Unknown	Yes	
WP_228085946.1	IB292_RS21975	Hcp	Cargo	Unknown	Unknown	Yes	

162

163 Constructing an “effectorless” surrogate T6SS platform

164 A surrogate T6SS platform can be used as a tool to study putative E/I pairs. The major advantage
 165 of the surrogate platform is that it only requires constructing a single plasmid to express the
 166 putative E/I pair in question (11). Since we have previously reported that the T6SS1 of POR1, a
 167 *V. parahaemolyticus* strain RIMD 2210633 derivative, can be used as a surrogate platform to
 168 deliver and investigate effectors and modules belonging to T6SS1 from other *V. parahaemolyticus*

169 strains (11), we decided to employ this strategy to investigate the putative DUF4225-containing
170 effector.

171 A drawback of our previously reported surrogate platform was the presence of the endogenous
172 T6SS1 effectors of the RIMD 2210633 strain (36), which prevented the use of a possibly sensitive
173 prey strain and thus required the use of a RIMD 2210633-derived strain containing the cognate
174 immunity proteins as prey during competition assays. To enable the use of a surrogate platform
175 during competition against diverse prey strains, we set out to construct an “effectorless” version.
176 To this end, we deleted the genes encoding the reported effector VPA1263 (36) and the co-
177 effector VP1388 (37), and we replaced two residues in the predicted active site of the specialized
178 effector VP1415 (36) with alanine, as previously reported (55). In addition, we deleted *vp1133*,
179 which encodes an H-NS protein that represses T6SS1 activity in *V. parahaemolyticus* (56), to
180 constitutively activate T6SS1 in the surrogate strain. The resulting platform, which we named
181 VpT6SS1^{Surrogate}, is active at 30°C in media containing 3% (wt/vol) NaCl, as evident by the
182 expression and secretion of the hallmark VgrG1 protein in a T6SS1-dependent manner
183 (**Supplementary Fig. S3A**). Furthermore, VpT6SS1^{Surrogate} enables interbacterial killing of
184 susceptible *V. natriegens* prey during competition mediated by a plasmid-borne VgrG1b auxiliary
185 module belonging to T6SS1 of *V. parahaemolyticus* strain 12-297/B, containing the PoNe DNase
186 effector (7) (**Supplementary Fig. S3B**).

187

188 **A DUF4225-containing protein is a T6SS1 antibacterial effector**

189 To determine whether DUF4225-encoding genes and their adjacent downstream genes are
190 antibacterial T6SS E/I pairs, we chose to investigate an Hcp auxiliary module from *V.*
191 *parahaemolyticus* strain CFSAN018764 (**Supplementary Fig. S2**; RefSeq sequence
192 NZ_LHBG01000025.1) encoding an Hcp and a DUF4225-containing protein, hereafter referred
193 to as DUF4225¹⁸⁷⁶⁴ (accession numbers WP_065788327.1 and WP_065788326.1, respectively).
194 This strain harbors both T6SS1 and T6SS2 (**Supplementary Dataset S2**). Since the module’s
195 Hcp is more similar to Hcp1 than to Hcp2 (**Supplementary Fig. S4** and **Supplementary Dataset**
196 **S5**), we reasoned that this Hcp auxiliary module is probably associated with T6SS1; we therefore
197 named this Hcp as Hcp1b.

198 The Hcp1b module lacked an annotated gene immediately downstream of the gene encoding the
199 putative effector DUF4225¹⁸⁷⁶⁴. Nevertheless, when we performed a manual analysis of the
200 nucleotide sequence, we identified an open reading frame immediately downstream of the
201 putative effector (positions 296 to 27 in NZ_LHBG01000025.1) (**Supplementary Fig. S2**). The
202 identified gene encodes an 89 amino acid-long protein containing three predicted transmembrane
203 helices. Therefore, we predicted that this gene encodes a cognate DUF4225¹⁸⁷⁶⁴ immunity
204 protein, and we named it Imm4225¹⁸⁷⁶⁴.

205 Using VpT6SS1^{Surrogate}, we next set out to investigate the ability of the Hcp1b auxiliary module
206 from strain CFSAN018764 to mediate T6SS1-dependent competition. As shown in **Figure 3**, an
207 arabinose-inducible plasmid encoding the three proteins of the Hcp1b module (pModule; i.e.,
208 Hcp1b, DUF4225¹⁸⁷⁶⁴, and Imm4225¹⁸⁷⁶⁴), but not Hcp1b alone (pHcp1b), mediated the T6SS1-
209 dependent intoxication of *V. natriegens* prey. Expression of Imm4225¹⁸⁷⁶⁴ from a plasmid (pImm)
210 rescued the *V. natriegens* prey strain from this attack. Taken together, these results indicate that
211 the Hcp1b auxiliary module of *V. parahaemolyticus* strain CFSAN018764 carries a T6SS1
212 antibacterial E/I pair.

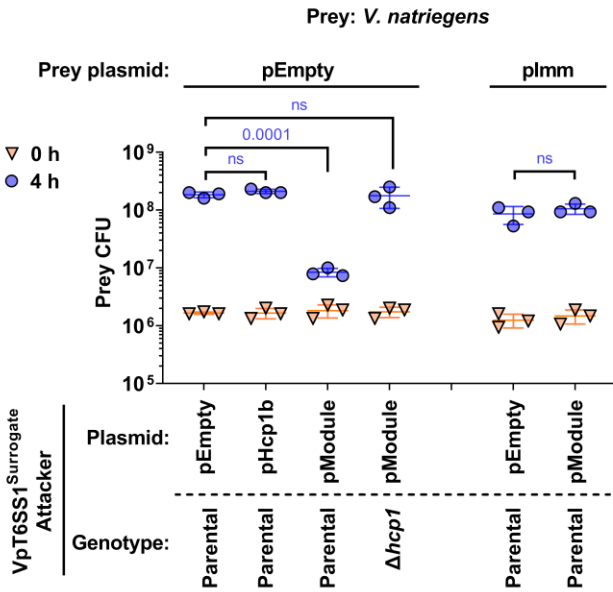


Figure 3. A DUF4225-containing Hcp auxiliary module contains a T6SS1 effector and immunity pair. Viability counts (CFU) of *V. natriegens* prey strains containing an empty plasmid (pEmpty) or a plasmid for the arabinose-inducible expression of Imm4225¹⁸⁷⁶⁴ (plmm) before (0 h) and after (4 h) co-incubation with the surrogate T6SS1 platform strain (VpT6SS1^{Surrogate}) or its T6SS1-derivative (Δ hcp1) carrying an empty plasmid (pEmpty) or a plasmid for the arabinose-inducible expression of Hcp1b (pHcp1b) or the three-gene Hcp1b module (pModule) from *V. parahaemolyticus* strain CFSAN018764. The statistical significance between samples at the 4 h timepoint was calculated using an unpaired, two-tailed Student's *t*-test; ns, no significant difference ($p > 0.05$). Data are shown as the mean \pm SD; $n = 3$.

213

214 A DUF4225-containing effector leads to cell lysis upon delivery to the periplasm

215 Next, we investigated the toxicity mediated by DUF4225¹⁸⁷⁶⁴. The arabinose-inducible expression
 216 of the effector in the periplasm of *E. coli* (by fusion to an N-terminal PelB signal peptide), but not
 217 in the cytoplasm, led to a clear reduction in the optical density (OD₆₀₀) of the bacterial culture over
 218 time (**Fig. 4A**); the phenotype was similar to the lytic effect of the amidase effector Tse1 from
 219 *Pseudomonas aeruginosa* (57), and dissimilar to the effect of the membrane-disrupting effector
 220 Tme1 from *V. parahaemolyticus* (11). Lysis was also observed when *E. coli* cells expressing the
 221 periplasmic version of DUF4225¹⁸⁷⁶⁴ were visualized under a fluorescence microscope.
 222 Approximately 90 minutes after inducing DUF4225¹⁸⁷⁶⁴ expression, cells began to shrink and
 223 appeared to have lost their cytoplasmic content. Concomitantly, the leakage of DNA from these
 224 cells became apparent, manifesting as the fluorescence of propidium iodide (PI), a non-
 225 permeable DNA dye that was added to the media, around them (**Fig. 4B** and **Supplementary**
 226 **Movie S1**). These phenotypes are characteristic of cell lysis (58). Sometimes, mostly at later
 227 stages of the time course, we observed cells stained from the inside by PI, indicative of the slow
 228 permeabilization of the membranes. Similar phenotypes were not seen in *E. coli* cells containing
 229 an empty expression plasmid (**Supplementary Fig. S5** and **Supplementary Movie S1**). Taken
 230 together, our results suggest that the activity of DUF4225¹⁸⁷⁶⁴ in the bacterial periplasm can lead
 231 to cell lysis. Importantly, the co-expression of Imm4225¹⁸⁷⁶⁴ in *E. coli* rescued the cells from the
 232 toxicity mediated by periplasmic DUF4225¹⁸⁷⁶⁴ (**Fig. 4C**), further supporting its role as the cognate
 233 immunity protein of this effector. The expression of the non-toxic cytoplasmic version of
 234 DUF4225¹⁸⁷⁶⁴ was detected in immunoblots, whereas the toxic periplasmic version of
 235 DUF4225¹⁸⁷⁶⁴ was only detected when Imm4225¹⁸⁷⁶⁴ was co-expressed (**Supplementary Fig.**
 236 **S6**).

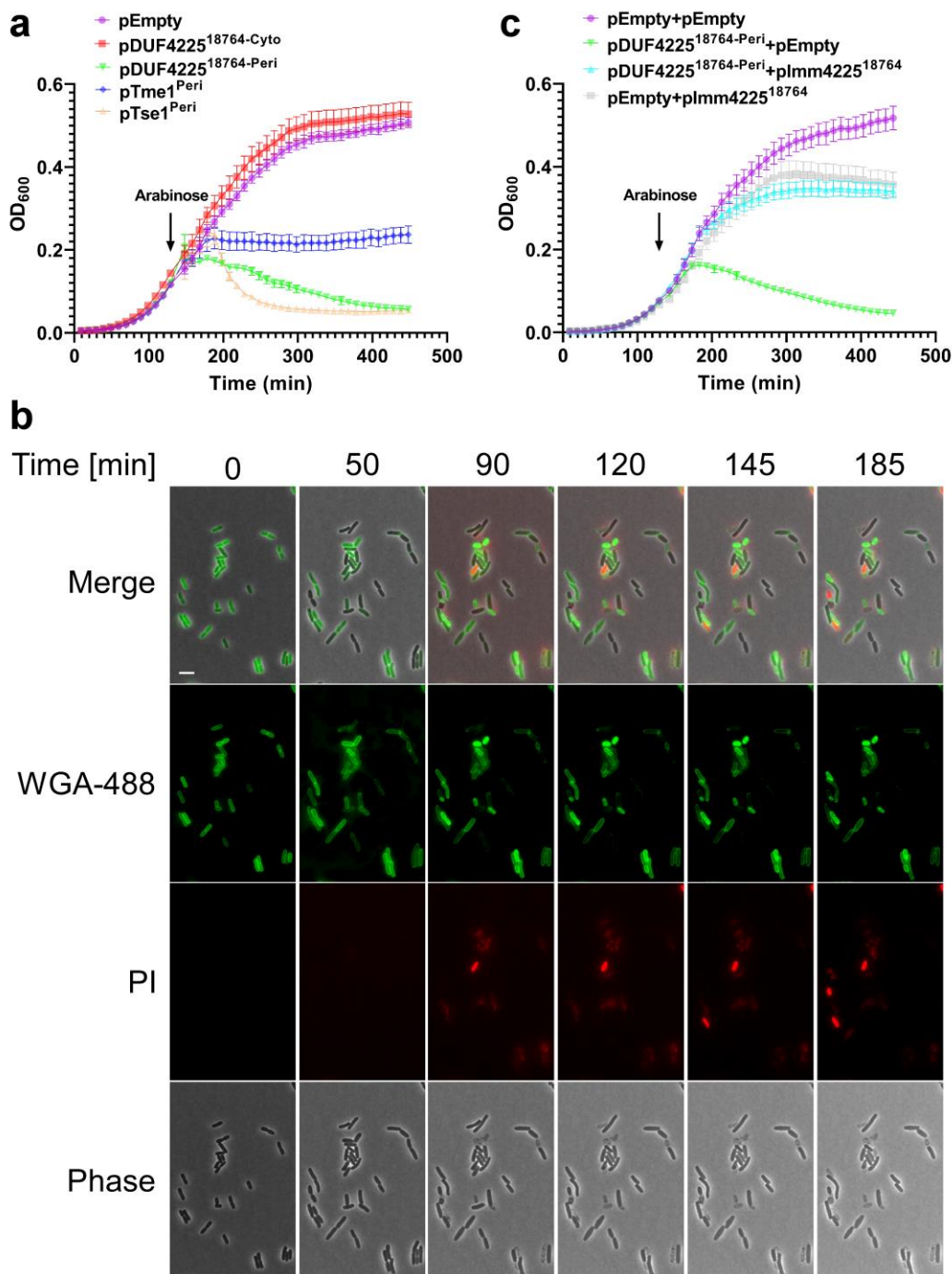


Figure 4. DUF4225¹⁸⁷⁶⁴ induces cell lysis upon delivery to the periplasm. (a,c) Growth of *E. coli* BL21 (DE3) containing arabinose-inducible plasmids, either empty (pEmpty) or expressing the indicated proteins in the cytoplasm (Cyto) or periplasm (Peri; fused to an N-terminal PelB signal peptide). In 'c', bacteria contain a second plasmid, either empty (pEmpty) or encoding Imm4225¹⁸⁷⁶⁴. An arrow denotes the timepoint at which arabinose (0.05%) was added to the media. (b) Time-lapse microscopy of *E. coli* MG1655 cells stained with Wheat Germ Agglutinin Alexa Fluor 488 conjugate (WGA-488) and that express a periplasmic DUF4225¹⁸⁷⁶⁴ from an arabinose-inducible plasmid, grown on agarose pads supplemented with chloramphenicol (to maintain the plasmid) and 0.2% arabinose (to induce expression), and propidium iodide (PI). WGA-488 (green), PI (red), phase contrast and merged channels are shown. Size bar = 5 μ m.

238 ***Vibrio* strains without a cognate immunity protein can resist DUF4225¹⁸⁷⁶⁴ toxicity**

239 We and others previously reported that certain T6SS effectors appear to have a specific toxicity
 240 range; they can intoxicate some but not all bacterial prey strains during T6SS-mediated attacks
 241 (55, 59). Since some resistant strains do not carry a homolog of the intoxicating effector's cognate
 242 immunity protein, it had been suggested that non-immunity protein-mediated defense
 243 mechanisms play a role in such resistance (60). In light of these recent observations, we set out
 244 to examine the toxicity range of a T6SS attack mediated by DUF4225¹⁸⁷⁶⁴. To this end, we
 245 monitored the viability of several marine bacteria prey strains during competition against the
 246 VpT6SS1^{Surrogate} platform delivering DUF4225¹⁸⁷⁶⁴. For prey strains with antibacterial T6SSs
 247 known or predicted to be active under the tested conditions, we used mutants in which the T6SS
 248 was inactivated by deleting a T6SS core component (e.g., *hcp* or *tssB*), as indicated, to avoid
 249 counterattacks during competition. Interestingly, whereas *V. campbellii* ATCC 25920, *V.*
 250 *coralliilyticus* ATCC BAA-450, and *Aeromonas jandaei* DSM 7311 were susceptible to a
 251 DUF4225¹⁸⁷⁶⁴-mediated attack, *V. parahaemolyticus* 12-297/B was only mildly susceptible to the
 252 attack and *V. vulnificus* CMCP6 and *V. parahaemolyticus* RIMD 2210633 were not affected by it
 253 (Fig. 5). The three latter strains do not carry a homolog of Imm4225¹⁸⁷⁶⁴. Importantly, all prey
 254 strains except for *V. parahaemolyticus* 12-297/B and *Aeromonas jandaei* DSM 7311, which
 255 contain a PoNi immunity protein, were susceptible to intoxication by a PoNe DNase effector from
 256 *V. parahaemolyticus* strain 12-297/B (7), when it was delivered by the VpT6SS1^{Surrogate} platform
 257 (Fig. 5); this result indicates that the platform can deliver effectors into the tested prey strains.
 258 Therefore, our results reveal that certain bacteria can resist intoxication by DUF4225¹⁸⁷⁶⁴ even in
 259 the absence of a cognate immunity protein.

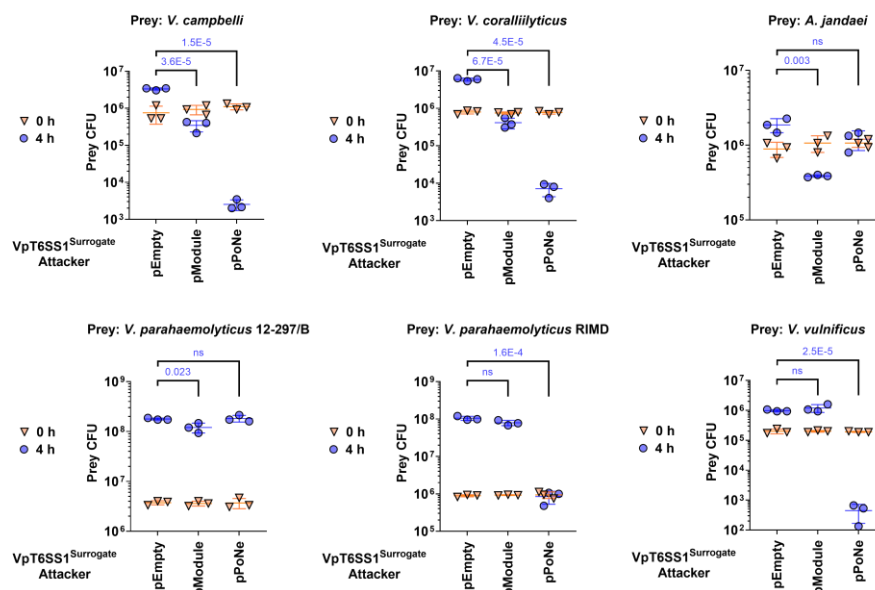


Figure 5. Varying sensitivity of marine bacteria to DUF4225¹⁸⁷⁶⁴ T6SS-mediated attacks. Viability counts (CFU) of the indicated prey strains before (0 h) and after (4 h) co-incubation with the surrogate T6SS1 platform strain (VpT6SS1^{Surrogate}) carrying an empty plasmid (pEmpty) or a plasmid for the arabinose-inducible expression of the three-gene Hcp1b module (pModule) from *V. parahaemolyticus* strain CFSAN018764 or the PoNe DNase-containing VgrG1b module from *V. parahaemolyticus* 12-297/B (pPoNe). Statistical significance between samples at the 4 h timepoint was calculated using an unpaired, two-tailed Student's *t*-test; ns, no significant difference ($P > 0.05$). Data are shown as the mean \pm SD; n=3. The prey strains used were *V. campbellii* ATCC 25920 Δ *hcp1*, *V. coralliilyticus* ATCC BAA-450 Δ *hcp1*, *Aeromonas jandaei* DSM 7311 Δ *tssB*, *V. parahaemolyticus* 12-297/B Δ *hcp1*, *V. parahaemolyticus* RIMD 2210633 Δ *hcp1*, and *V. vulnificus* CMCP6.

260

261 **DUF4225 is a widespread toxin domain associated with diverse secretion systems**

262 We next investigated the distribution of the DUF4225 toxin domain in bacterial genomes. We
 263 found that the homologs of DUF4225¹⁸⁷⁶⁴ are widespread in bacterial genomes, almost
 264 exclusively belonging to the Pseudomonadota (formerly, Proteobacteria) phylum (**Fig. 6A** and
 265 **Supplementary Dataset S6**). Interestingly, DUF4225 is found in polymorphic toxins containing
 266 N-terminal domains associated with T6SS (e.g., PAAR, VgrG, and Hcp), type V secretion system
 267 (e.g., Fil_haemagg_2 and DUF637 (61)), and others (e.g., SpvB (53), RHS_repeat (16), and Sec
 268 system signal peptides), although most of the homologs do not contain an identifiable N-terminal
 269 domain fused to DUF4225 (**Fig. 6B** and **Supplementary Dataset S6**). Sometimes the association
 270 of the DUF4225-containing protein with a specific secretion system can be inferred from adjacent
 271 genes encoding known components of protein secretion systems, as is the case with
 272 DUF4225¹⁸⁷⁶⁴, which is encoded downstream of *hcp1b*. Taken together, these results reveal that
 273 DUF4225 is a toxin domain that is widespread in secreted polymorphic effectors.

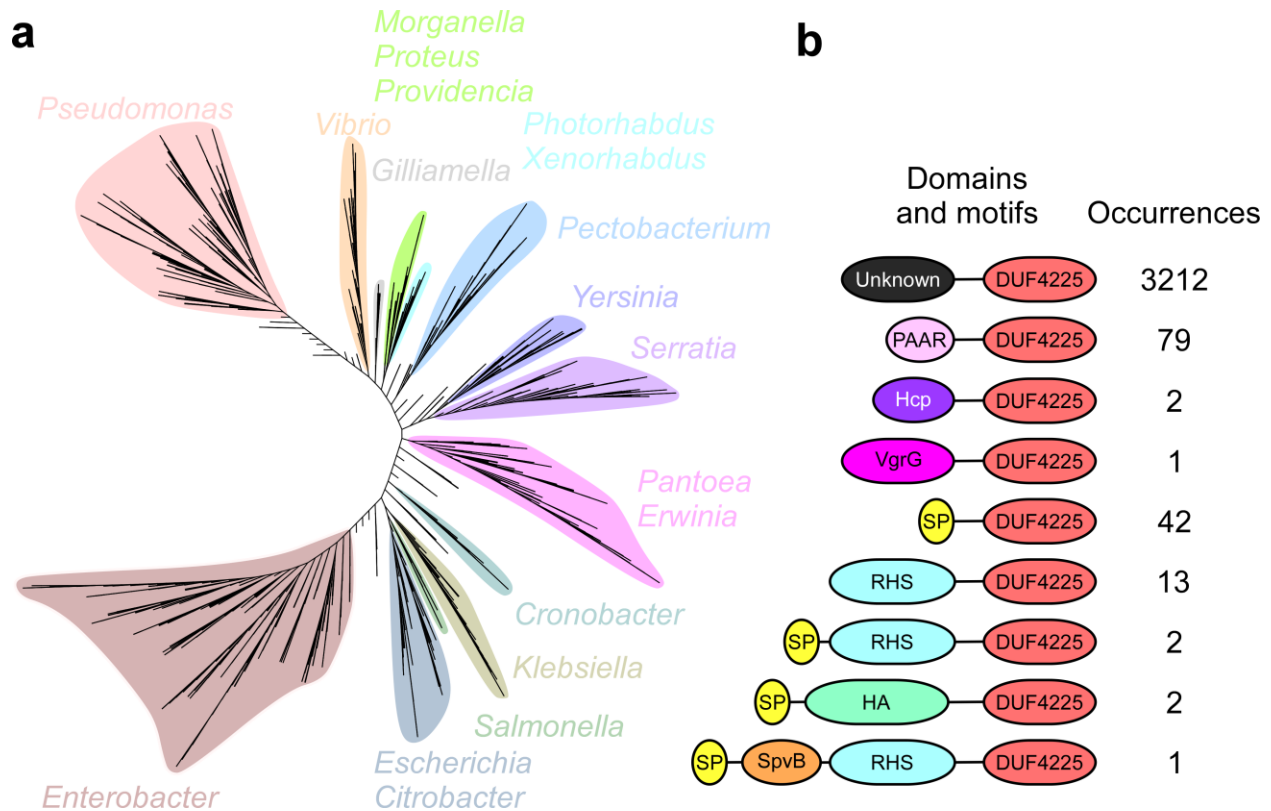


Figure 6. DUF4225 is a widespread toxin domain. (a) Phylogenetic distribution of bacteria encoding a DUF4225 homolog was based on the DNA sequences of *rpoB* coding for DNA-directed RNA polymerase subunit beta. The evolutionary history was inferred using the neighbor-joining method. **(b)** The domain architecture and the number of occurrences of DUF4225-containing proteins. SP, signal peptide; HA, Haemagg_act + Fil_haemagg_2 + DUF637. Domain sizes are not to scale.

274

275 **Discussion**

276 *V. parahaemolyticus* is an emerging marine pathogen responsible for gastroenteritis in humans
 277 (40) and for the economically devastating acute hepatopancreatic necrosis disease in shrimp (62).
 278 Like many other vibrios, this species employs T6SSs to manipulate and outcompete its rivals (7,

279 11, 43, 45). Here, we performed a systematic analysis of all available RefSeq *V. parahaemolyticus*
280 genomes, and we revealed the pan-genome repertoire of T6SS gene clusters, auxiliary modules,
281 and the effectors therein.

282 We identified four T6SS gene cluster types in *V. parahaemolyticus* genomes. Two systems
283 appear to be ancient and widespread, and two seem to have been more recently acquired. T6SS1
284 and T6SS2, which were previously shown to mediate antibacterial activities (11, 43), are the most
285 common systems in this species. T6SS2 is omnipresent; therefore, it is probably an ancient
286 system that plays an important role in the *V. parahaemolyticus* life cycle. T6SS1, which is present
287 in 68.3% of the genomes, is possibly also an ancient system; however, since T6SS1 appears to
288 be absent from certain lineages (**Fig. 2**), we propose that it had been lost several times during
289 the evolution of this species. This may be because T6SS1 serves a specialized purpose that is
290 not beneficial for some strains. Indeed, we and others previously proposed that T6SS1 is present
291 predominantly in pathogenic isolates of *V. parahaemolyticus* (41–43); therefore, it is plausible that
292 non-pathogenic strains have lost this system, since it may only be required during colonization of
293 a host. T6SS3 and T6SS4 are found in <3% of the genomes combined. Since DNA mobility genes
294 flank these gene clusters, we propose that they have been recently acquired via HGT. This seems
295 possible in light of the ability of vibrios to horizontally acquire large DNA fragments (46, 63, 64).
296 The role and activity mediated by these two systems remains to be investigated. Nevertheless,
297 we propose that T6SS3 mediates anti-eukaryotic activity, since it is similar to the previously
298 reported T6SS3 in *V. proteolyticus* (50), and since we identified a putative effector within the
299 cluster that lacks an identifiable potential immunity protein, suggesting that it does not mediate
300 antibacterial activity. We also propose that T6SS4 mediates antibacterial activities, since we
301 identified putative antibacterial effectors within it, which have a downstream adjacent gene that
302 possibly encodes a cognate immunity protein (**Fig. 1b** and **Table 1**).

303 Our analysis also revealed diverse T6SS auxiliary modules encoding at least one of the secreted
304 proteins, Hcp, VgrG, and PAAR. In most of these auxiliary modules, we found known or putative
305 effectors that can diversify the toxic repertoires of this species' T6SSs. The identity of these genes
306 as effectors is supported by their homology to known effectors, by their position downstream of
307 genes encoding T6SS adaptors, by the presence of domains associated with T6SS-secreted
308 proteins (e.g., MIX (36) and FIX (7)), and by the presence of homologs of their C-terminus in
309 polymorphic toxins (**Table 1**). Interestingly, several effectors, identified within auxiliary modules,
310 do not resemble previously studied toxins, and they may therefore employ novel mechanisms of
311 action. Notably, although this was not directly addressed in this work, additional orphan effectors
312 have been previously reported in *V. parahaemolyticus* genomes (7, 11, 42, 45); many are found
313 next to DNA mobility genes, suggesting that they may also be horizontally shared within this
314 species (42, 48). These orphan effectors further diversify the T6SS effector repertoire of this
315 species.

316 In this work, we investigated the role of a gene encoding a DUF4225-containing protein; we
317 showed that it is an antibacterial T6SS1 effector, and that its cognate immunity protein is encoded
318 directly downstream. To the best of our knowledge, this is the first activity described for this
319 domain of unknown function. Notably, DUF4225-encoding genes are common in Hcp-containing
320 auxiliary modules, suggesting that they too are T6SS effectors. Our analysis also revealed that
321 DUF4225 is widespread outside vibrios, where it is associated with T6SSs, as well as with other
322 secretion systems that deliver polymorphic toxins.

323 We found that DUF4225 exerts its toxic activity in the bacterial periplasm. However, its
324 mechanism of action and its cellular target remain unknown. Since its expression in the periplasm
325 of *E. coli* cells led to cell lysis, we hypothesize that it affects the stability of the peptidoglycan or
326 the membrane. Future biochemical and structural work will be required to address these open
327 questions. Interestingly, we identified marine bacteria that resist intoxication by a DUF4225-

328 containing effector. Since we did not identify homologs of the cognate immunity protein encoded
329 within the genomes of these resistant strains, we predict that they employ a yet-unknown non-
330 immunity protein-mediated defense mechanism that counteracts the toxicity of this effector.

331 The effectorless surrogate T6SS platform constructed in this work is an important tool, allowing
332 us to rapidly identify and investigate T6SS effectors encoded by any *V. parahaemolyticus* strain.
333 Although we previously reported the construction of a similar surrogate system (11), the
334 effectorless version reported here is superior: 1) the toxicity mediated by a putative effector can
335 be tested against diverse prey strains, thus reducing the possibility of false negatives due to the
336 lack of toxicity against a *V. parahaemolyticus* RIMD 2210633 prey (in hindsight, DUF4225¹⁸⁷⁶⁴
337 would have been a false negative in the previous version of the surrogate platform); and 2) no
338 endogenous effectors compete with the investigated putative effector for loading onto the
339 secreted tube and spike, thus increasing the probability that it will be delivered by the surrogate
340 system.

341 In conclusion, we present the first comprehensive analysis of the T6SS repertoire in the *V.*
342 *parahaemolyticus* pan-genome. Our results reveal four T6SSs found within this species; they also
343 indicate that mobile auxiliary modules probably contribute greatly to diversifying the T6SS effector
344 repertoires in various strains. We also describe a role for the widespread DUF4225 as an
345 antibacterial toxin domain, and we identify additional putative effectors that await investigation.

346

347 **Materials and Methods**

348 **Strains and Media:** For a complete list of strains used in this study, see [Supplementary Table](#)
349 [S1](#). *E. coli* strains were grown in 2xYT broth (1.6% wt/vol tryptone, 1% wt/vol yeast extract, and
350 0.5% wt/vol NaCl) or on Lysogeny Broth (LB) agar plates containing 1% wt/vol NaCl at 37°C, or
351 at 30°C when harboring effector expression plasmids. The media were supplemented with
352 chloramphenicol (10 µg/mL) or kanamycin (30 µg/mL) to maintain plasmids, and with 0.4% wt/vol
353 glucose to repress protein expression from the arabinose-inducible promoter, *Pbad*. To induce
354 expression from *Pbad*, L-arabinose was added to the media at 0.1-0.2% (wt/vol), as indicated.

355 *Vibrio parahaemolyticus*, *V. natriegens*, *V. coralliilyticus*, and *V. vulnificus* strains were grown in
356 MLB media (LB media containing 3% wt/vol NaCl) or on marine minimal media (MMM) agar plates
357 (1.5% wt/vol agar, 2% wt/vol NaCl, 0.4% wt/vol galactose, 5 mM MgSO₄, 7 mM K₂SO₄, 77 mM
358 K₂HPO₄, 35 mM KH₂PO₄, and 2 mM NH₄Cl). *V. campbellii* were grown in MLB media and on MLB
359 agar plates. *Aeromonas jandaei* were grown in LB media and on LB agar plates. When vibrios or
360 *A. jandaei* contained a plasmid, the media were supplemented with kanamycin (250 µg/mL),
361 chloramphenicol (10 µg/mL), or streptomycin (100 µg/mL) to maintain the plasmid. Bacteria were
362 grown at 30°C. To induce expression from *Pbad*, L-arabinose was added to media at 0.05%
363 (wt/vol).

364 **Plasmid construction:** For a complete list of plasmids used in this study, see [Supplementary](#)
365 [Table S2](#). The DNA sequence of the Hcp1b auxiliary module from *V. parahaemolyticus* strain
366 CFSAN018764 (positions 296 to 27 in NZ_LHBG01000025.1) was synthesized by Twist
367 Bioscience (USA). The entire module sequence or the sequences of genes within it were PCR
368 amplified and then inserted into the multiple cloning site (MCS) of pBAD^K/Myc-His, pPER5, or
369 pBAD33.1^F, in-frame with C-terminal Myc-His or FLAG tags, using the Gibson assembly method
370 (65). For the expression of Imm4225¹⁸⁷⁶⁴ in *V. natriegens*, the region spanning the *araC* gene to
371 the *rrnT1* terminator was amplified from pBAD33.1^F containing the gene in its MCS, and then
372 inserted into the *NotI* restriction site of pCLTR plasmid using restriction-digestion and ligation.

373 Plasmids were introduced into *E. coli* using electroporation. Transformants were grown on agar
374 plates supplemented with 0.4% wt/vol glucose to repress expression from the *Pbad* promoter

375 during the subcloning steps. Plasmids were introduced into vibrios and *A. jandaei* via conjugation.
376 Trans-conjugants were grown on MLB agar plates for *V. campbellii*, LB agar plates for *A. jandaei*,
377 or MMM agar plates for all other vibrios. Plates were supplemented with appropriate antibiotics to
378 maintain the plasmids.

379 **Construction of deletion strains:** For in-frame deletions of *hcp1* in *V. corallilyticus*
380 (VIC_RS16330) or of *hcp1* in *V. campbellii* (A8140_RS17660), 1 kb sequences upstream and
381 downstream of each gene were subcloned into pDM4, a Cm^rOriR6K suicide plasmid (66). Next,
382 pDM4 constructs were introduced into the respective *Vibrio* strain via conjugation. Trans-
383 conjugants were selected on MMM agar plates containing chloramphenicol (10 µg/mL). The
384 resulting trans-conjugants were grown on MMM agar plates containing sucrose (15% wt/vol) for
385 counter-selection and loss of the SacB-containing pDM4.

386 The VpT6SS1^{Surrogate} strain and its Δ *hcp1* derivative were generated by consecutive deletions or
387 mutations of the relevant genes using previously reported pDM4 plasmids.

388 **Toxicity assays in *E. coli*:** To assess the toxicity mediated by DUF4225¹⁸⁷⁶⁴, pBAD^K/Myc-His
389 (for cytoplasmic expression) and pPER5 (for periplasmic expression fused to an N-terminal PelB
390 signal peptide) plasmids, either empty or encoding DUF4225¹⁸⁷⁶⁴ were transformed into *E. coli*
391 BL21 (DE3). *E. coli* transformants were grown overnight in 2xYT media supplemented with
392 kanamycin (30 µg/mL) under *Pbad* repressing conditions (0.4% wt/vol glucose). Overnight
393 cultures were washed to remove residual glucose, and normalized to OD₆₀₀ = 0.01 in 2xYT media
394 supplemented with kanamycin. Then, 200 µL of each bacterial culture were transferred into 96-
395 well plates in quadruplicate. The cultures were grown at 37 °C with agitation (205 cpm) in a
396 microplate reader (BioTek SYNERGY H1). After 2 h of growth, L-arabinose was added to each
397 well at a final concentration of 0.1% (wt/vol), to induce protein expression. OD₆₀₀ readings were
398 recorded every 10 min for 7 h.

399 To test the ability of Imm4225¹⁸⁷⁶⁴ to antagonize the toxicity of DUF4225¹⁸⁷⁶⁴, a pBAD33.1^F
400 plasmid, either empty or encoding Imm4225¹⁸⁷⁶⁴, was co-transformed with a pPER5 plasmid,
401 either empty or encoding DUF4225¹⁸⁷⁶⁴, into *E. coli* BL21 (DE3). The growth of these strains was
402 determined as described above. Growth assays were performed at least four times with similar
403 results. Results from a representative experiment are shown.

404 **Protein expression in *E. coli*:** To determine the expression of C-terminal Myc-His-tagged
405 DUF4225¹⁸⁷⁶⁴, *E. coli* BL21 (DE3) bacteria carrying a single arabinose-inducible expression
406 plasmid, either empty or encoding a cytoplasmic or a periplasmic DUF4225¹⁸⁷⁶⁴, or bacteria
407 carrying two plasmids, one for expression of Imm4225¹⁸⁷⁶⁴ and the other either empty or
408 expressing the periplasmic version of DUF4225¹⁸⁷⁶⁴, were grown overnight in 2xYT media
409 supplemented with the appropriate antibiotics to maintain plasmids, and glucose to repress
410 expression from *Pbad*. The cultures were washed twice with fresh 2xYT medium to remove
411 residual glucose, and then diluted 100-fold in 5 mL of fresh 2xYT medium supplemented with
412 appropriate antibiotics and grown for 2 h at 37°C. To induce protein expression, 0.1% (wt/vol) L-
413 arabinose was added to the media. After 4 additional hours of growth at 30°C, 1.0 OD₆₀₀ units of
414 cells were pelleted and resuspended in 100 µL of (2X) Tris-Glycine SDS sample buffer (Novex,
415 Life Sciences). Samples were boiled for 5 min, and cell lysates were resolved on Mini-
416 PROTEAN TGX Stain-Free™ precast gels (Bio-Rad). For immunoblotting, α-Myc antibodies
417 (Santa Cruz Biotechnology, 9E10, mouse mAb; sc-40) were used at 1:1,000 dilution. Protein
418 signals were visualized in a Fusion FX6 imaging system (Vilber Lourmat) using enhanced
419 chemiluminescence (ECL) reagents. Experiments were performed at least three times with similar
420 results; the results from representative experiments are shown.

421 **Bacterial competition assays:** Bacterial competition assays were performed as previously
422 described (37), with minor changes. Briefly, cultures of the indicated attacker and prey strains

423 were grown overnight. Bacterial cultures were then normalized to $OD_{600} = 0.5$ and mixed at a 10:1
424 (attacker: prey) ratio. The mixtures were spotted (25 μ L) on MLB agar plates supplemented with
425 0.05% (wt/vol) L-arabinose, and incubated for 4 h at 30°C. Colony forming units (CFU) of the prey
426 strains were determined at the 0 and 4-hour timepoints. The experiments were performed at least
427 three times with similar results. Results from a representative experiment are shown.

428 **Fluorescence microscopy:** Cell morphology and membrane permeability during the expression
429 of DUF4225¹⁸⁷⁶⁴ in *E. coli* was assessed as previously described (37). Briefly, overnight-grown
430 *E. coli* MG1655 cells carrying a pPER5 plasmid, either empty or encoding DUF4225¹⁸⁷⁶⁴, were
431 diluted 100-fold into 5 mL of fresh LB media supplemented with kanamycin and 0.2% (wt/vol)
432 glucose. Bacterial cultures were grown for 2 h at 37°C, and then cells were washed with 0.15 M
433 NaCl to remove residual glucose. Bacterial cultures were normalized to $OD_{600} = 0.5$ in 0.15 M
434 NaCl solution. To visualize the cell wall of *E. coli*, 20 μ L of bacterial cultures were incubated with
435 Wheat Germ Agglutinin Alexa Fluor 488 Conjugate (Biotium; Catalogue no. 29022–1) at a final
436 concentration of 0.1 mg/mL, and incubated for 10 min at room temperature (RT). Next, 1 μ L was
437 spotted on LB agarose pads (1% wt/vol agarose supplemented with 0.2% wt/vol L-arabinose)
438 onto which 1 μ L of the membrane-impermeable DNA dye, propidium iodide (PI; 1 mg/mL; Sigma-
439 Aldrich) had been pre-applied. After the spots had dried (1–2 min at RT), the agarose pads were
440 mounted, facing down, on 35 mm glass bottom CELLview™ cell culture dishes (Greiner). Cells
441 were then imaged every 5 min for 4 h under a fluorescence microscope, as detailed below. The
442 stage chamber (Okolab) temperature was set to 37°C. Bacteria were imaged in a Nikon Eclipse
443 Ti2-E inverted motorized microscope equipped with a CFI PLAN apochromat DM 100X oil lambda
444 PH-3 (NA, 1.45) objective lens, a Lumencor SOLA SE II 395 light source, and ET-EGFP (#49002,
445 used to visualize the Alexa Fluor 488 signal), and an RFP filter cube (#49005, used to visualize
446 the PI signal) filter sets. Images were acquired using a DS-QI2 Mono cooled digital microscope
447 camera (16 MP) and were post-processed using Fiji ImageJ suite. The experiments were
448 performed three times. Results from a representative experiment are shown.

449 **VgrG1 secretion assays:** *V. parahaemolyticus* VpT6SS1^{Surrogate} and its $\Delta hcp1$ derivative strain
450 were grown overnight at 30°C in MLB media. Bacterial cultures were normalized to $OD_{600} = 0.18$
451 in 5 mL of MLB media, and after 5 h of incubation at 30°C with agitation (220 rpm), expression
452 fractions (cells) and secretion fractions (media) were collected and processed as previously
453 described (37).

454 **Identifying T6SS gene clusters in *V. parahaemolyticus*:** A local database containing the
455 RefSeq bacterial nucleotide and protein sequences was generated (last updated on June 11,
456 2022). *V. parahaemolyticus* genomes were retrieved from the local database and OrthoANI was
457 performed as described previously (11, 67). Two genomes (assembly accessions
458 GCF_000591535.1 and GCF_003337295.1) with OrthoANI values <95% were removed from the
459 dataset.

460 The presence of T6SS gene clusters in *V. parahaemolyticus* genomes was determined by
461 following the two-step procedure described below. In the first step, BLASTN (68) was employed
462 to align *V. parahaemolyticus* nucleotide sequences against the nucleotide sequences of
463 representative T6SS clusters ([Figure 1](#) and [Supplementary Dataset S3](#)). The expect value
464 threshold was set to 10^{-12} and the minimal alignment length was 500 bp. The results were then
465 sorted by their nucleotide accession numbers and bit score values (from largest to smallest), and
466 the best alignments for each nucleotide accession number were saved. This step resulted in a list
467 of *V. parahaemolyticus* nucleotide accession numbers and their best alignments to the
468 representative T6SS gene clusters, including the positions of the alignments. In the second step,
469 a two-dimensional matrix was generated for each T6SS gene cluster in which rows represented
470 the *V. parahaemolyticus* genomes and columns represented the coordinates of the specific T6SS
471 gene cluster. The matrices were then filled in with the percent identity values, based on the

472 positions of the alignments. Finally, the overall coverage was calculated for each T6SS gene
473 cluster in each genome. *V. parahaemolyticus* genomes with at least 70% overall coverage of
474 T6SS gene cluster were regarded as containing that T6SS gene cluster ([Supplementary Dataset](#)
475 [S3](#)).

476 **Identifying T6SS auxiliary modules:** RPS-BLAST (69) was employed to identify proteins
477 containing Hcp (COG3157), PAAR (DUF4150, PAAR_motif, PAAR_1, PAAR_2, PAAR_3,
478 PAAR_4, PAAR_5, PAAR_RHS, PAAR_CT_1, PAAR_CT_2), and VgrG (COG3501) domains
479 that were retrieved from the Conserved Domain Database (70), in *V. parahaemolyticus* genomes.
480 Protein accessions located at the ends of contigs were removed. T6SS auxiliary modules were
481 manually identified, based on the distance from the T6SS gene clusters, the genomic architecture,
482 and the conserved domains in neighboring genes ([Supplementary Dataset S4](#)).

483 **Identifying DUF4225 homologs with domain and neighborhood analysis:** The Position-
484 Specific Scoring Matrix (PSSM) of the DUF4225 domain was reconstructed using amino acids
485 105-243 of DUF4225¹⁸⁷⁶⁴ from *V. parahaemolyticus* strain CFSAN018764 (WP_065788326.1).
486 Five iterations of PSI-BLAST were performed against the reference protein database (a maximum
487 of 500 hits with an expect value threshold of 10^{-6} and a query coverage of 70% were used in each
488 iteration). RPS-BLAST was then performed to identify DUF4225-containing proteins. The results
489 were filtered using an expect value threshold of 10^{-8} and a minimal coverage of 70%. The genomic
490 neighborhoods of DUF4225-containing proteins were analyzed as described previously (11, 45).
491 Duplicated protein accessions appearing in the same genome in more than one genomic
492 accession were removed if the same downstream protein existed at the same distance
493 ([Supplementary Dataset S6](#)).

494 **Constructing phylogenetic trees:** The nucleotide sequences of *rpoB* coding for DNA-directed
495 RNA polymerase subunit beta were retrieved from the local RefSeq database. Partial and
496 pseudogene sequences were not included in the analyses. In the case of bacterial genomes
497 encoding DUF4225 homologs, the *rpoB* sequences were first clustered using CD-HIT to remove
498 identical sequences (100% identity threshold). Phylogenetic analyses of bacterial genomes were
499 conducted using the MAFFT 7 server (mafft.cbrc.jp/alignment/server/). The *rpoB* sequences were
500 aligned using MAFFT v7 FFT-NS-2 (71, 72). In the case of *V. parahaemolyticus* genomes, the
501 evolutionary history was inferred using the neighbor-joining method (73) with the Jukes-Cantor
502 substitution model (JC69). The analysis included 1,694 nucleotide sequences and 3,964
503 conserved sites. In the case of bacterial genomes encoding DUF4225, the evolutionary history
504 was inferred using the average linkage (UPGMA) method and included 2,816 nucleotide
505 sequences.

506 The protein accessions of TssB and Hcp from *V. parahaemolyticus* genomes were retrieved and
507 unique sequences were aligned using CLUSTAL Omega (74). The evolutionary history was
508 inferred using the Neighbor-Joining method (73). The analysis of TssB included 42 amino acid
509 sequences and 166 conserved sites. The analysis of Hcp included 27 amino acid sequences and
510 133 conserved sites. Evolutionary analyses in both cases were conducted in MEGA X (75).

511 **Identifying effectors in T6SS gene clusters and auxiliary modules:** The presence of effectors
512 in T6SS gene clusters and auxiliary modules was determined by homology to previously studied
513 effectors in *V. parahaemolyticus*, by the location within auxiliary modules downstream of secreted
514 core components (i.e., Hcp, VgrG, or PAAR) or of known T6SS adaptor-encoding genes (i.e.,
515 DUF4123, DUF1795, or DUF2169), and by the presence of potential C-terminal toxin domains
516 identified using NCBI's Conserved Domain Database (76). The presence of homologs of C-
517 terminal toxin domains in other polymorphic toxin classes was determined using Jackhmmer (77).

518

519 **Acknowledgments**

520 This project received funding from the European Research Council under the European Union's
521 Horizon 2020 research and innovation program (grant agreement no. 714224 to D Salomon), and
522 from the Israel Science Foundation (grant no. 920/17 to D Salomon, and grant no. 1362/21 to D
523 Salomon and E Bosis). CM Fridman was supported by scholarships from the Clore Israel
524 Foundation and from the Manna Center Program in Food Safety and Security at Tel Aviv
525 University, as well as by a scholarship for outstanding doctoral students from the Orthodox
526 community from the Council for Higher Education. We thank Hila Saar, Nikol Dvir, and Nely Altshul
527 for their excellent technical assistance, and members of the Salomon and Bosis laboratories for
528 helpful discussions and suggestions.

529

530 **Author Contributions**

531 B Jana: conceptualization, investigation, methodology, and writing—review and editing.

532 K Keppel: investigation and methodology

533 CM Fridman: investigation and methodology

534 E Bosis: conceptualization, funding acquisition, investigation, methodology, and writing—
535 original draft.

536 D Salomon: conceptualization, supervision, funding acquisition, investigation, methodology, and
537 writing—original draft.

538

539 **Conflict of Interest**

540 The authors declare that they have no conflict of interest.

541

542 **References**

- 543 1. Klein TA, Ahmad S, Whitney JC. 2020. Contact-dependent interbacterial antagonism
544 mediated by protein secretion machines. *Trends Microbiol.* Elsevier Ltd
545 <https://doi.org/10.1016/j.tim.2020.01.003>.
- 546 2. Hood RD, Singh P, Hsu FS, Güvener T, Carl MA, Trinidad RRS, Silverman JM, Ohlson
547 BB, Hicks KG, Plemel RL, Li M, Schwarz S, Wang WY, Merz AJ, Goodlett DR, Mougous
548 JD. 2010. A type VI secretion system of *Pseudomonas aeruginosa* targets a toxin to
549 bacteria. *Cell Host Microbe* 7:25–37.
- 550 3. Boyer F, Fichant G, Berthod J, Vandenbrouck Y, Attree I. 2009. Dissecting the bacterial
551 type VI secretion system by a genome wide in silico analysis: What can be learned from
552 available microbial genomic resources? *BMC Genomics* 10:104.
- 553 4. Bingle LE, Bailey CM, Pallen MJ. 2008. Type VI secretion: a beginner's guide. *Curr Opin*
554 *Microbiol* 11:3–8.
- 555 5. Wang J, Brackmann M, Castaño-Díez D, Kudryashev M, Goldie KN, Maier T, Stahlberg
556 H, Basler M. 2017. Cryo-EM structure of the extended type VI secretion system sheath-
557 tube complex. *Nat Microbiol* 2:1507–1512.
- 558 6. Shneider MM, Buth SA, Ho BT, Basler M, Mekalanos JJ, Leiman PG. 2013. PAAR-repeat
559 proteins sharpen and diversify the type VI secretion system spike. *Nature* 500:350–353.

- 560 7. Jana B, Fridman CM, Bosis E, Salomon D. 2019. A modular effector with a DNase
561 domain and a marker for T6SS substrates. *Nat Commun* 10:3595.
- 562 8. Crisan C V., Chande AT, Williams K, Raghuram V, Rishishwar L, Steinbach G, Watve
563 SS, Yunker P, Jordan IK, Hammer BK. 2019. Analysis of *Vibrio cholerae* genomes
564 identifies new type VI secretion system gene clusters. *Genome Biol* 20.
- 565 9. Hachani A, Allsopp LP, Oduko Y, Filloux A. 2014. The VgrG proteins are “à la carte”
566 delivery systems for bacterial type VI effectors. *J Biol Chem* 289:17872–84.
- 567 10. Russell AB, Leroux M, Hathazi K, Agnello DM, Ishikawa T, Wiggins PA, Wai SN,
568 Mougous JD. 2013. Diverse type VI secretion phospholipases are functionally plastic
569 antibacterial effectors. *Nature* 496:508–512.
- 570 11. Fridman CM, Keppel K, Gerlic M, Bosis E, Salomon D. 2020. A comparative genomics
571 methodology reveals a widespread family of membrane-disrupting T6SS effectors. *Nat*
572 *Commun* 11:1085.
- 573 12. Russell AB, Singh P, Brittnacher M, Bui NK, Hood RD, Carl MA, Agnello DM, Schwarz S,
574 Goodlett DR, Vollmer W, Mougous JD. 2012. A widespread bacterial type VI secretion
575 effector superfamily identified using a heuristic approach. *Cell Host Microbe* 11:538–549.
- 576 13. Jana B, Salomon D. 2019. Type VI secretion system: a modular toolkit for bacterial
577 dominance. *Future Microbiol* 14:fmb-2019-0194.
- 578 14. Basler M, Pilhofer M, Henderson GP, Jensen GJ, Mekalanos JJ. 2012. Type VI secretion
579 requires a dynamic contractile phage tail-like structure. *Nature* 483:182–6.
- 580 15. Ma LS, Hachani A, Lin JS, Filloux A, Lai EM. 2014. *Agrobacterium tumefaciens* deploys a
581 superfamily of type VI secretion DNase effectors as weapons for interbacterial
582 competition in planta. *Cell Host Microbe* 16:94–104.
- 583 16. Koskiniemi S, Lamoureux JG, Nikolakakis KC, t’Kint de Roodenbeke C, Kaplan MD, Low
584 DA, Hayes CS. 2013. Rhs proteins from diverse bacteria mediate intercellular
585 competition. *Proc Natl Acad Sci U S A* 110:7032–7.
- 586 17. Pissaridou P, Allsopp LP, Wettstadt S, Howard SA, Mavridou DAI, Filloux A. 2018. The
587 *Pseudomonas aeruginosa* T6SS-VgrG1b spike is topped by a PAAR protein eliciting DNA
588 damage to bacterial competitors. *Proc Natl Acad Sci U S A* 115:12519–12524.
- 589 18. Alcoforado Diniz J, Coulthurst SJ. 2015. Intraspecies competition in *Serratia marcescens*
590 is mediated by type VI-secreted Rhs effectors and a conserved effector-associated
591 accessory protein. *J Bacteriol* 197:2350–60.
- 592 19. Ma J, Pan Z, Huang J, Sun M, Lu C, Yao H. 2017. The Hcp proteins fused with diverse
593 extended-toxin domains represent a novel pattern of antibacterial effectors in type VI
594 secretion systems. *Virulence* 8:1189–1202.
- 595 20. LaCourse KD, Peterson SB, Kulasekara HD, Radey MC, Kim J, Mougous JD. 2018.
596 Conditional toxicity and synergy drive diversity among antibacterial effectors. *Nat*
597 *Microbiol* 3:440–446.
- 598 21. Mariano G, Trunk K, Williams DJ, Monlezun L, Strahl H, Pitt SJ, Coulthurst SJ. 2019. A
599 family of Type VI secretion system effector proteins that form ion-selective pores. *Nat*
600 *Commun* 10:1–15.
- 601 22. Miyata ST, Unterweger D, Rudko SP, Pukatzki S. 2013. Dual expression profile of type VI
602 secretion system immunity genes protects pandemic *Vibrio cholerae*. *PLoS Pathog* 9:1–
603 18.

- 604 23. Whitney JC, Chou S, Russell AB, Biboy J, Gardiner TE, Ferrin MA, Brittnacher M,
605 Vollmer W, Mougous JD. 2013. Identification, structure, and function of a novel type VI
606 secretion peptidoglycan glycoside hydrolase effector-immunity pair. *J Biol Chem*
607 288:26616–24.
- 608 24. Sibinelli-Sousa S, Hespanhol JT, Nicastro GG, Matsuyama BY, Mesnage S, Patel A, de
609 Souza RF, Guzzo CR, Bayer-Santos E. 2020. A family of T6SS antibacterial effectors
610 related to I,d-transpeptidases targets the peptidoglycan. *Cell Rep* 31:107813.
- 611 25. Whitney JC, Quentin D, Sawai S, LeRoux M, Harding BN, Ledvina HE, Tran BQ,
612 Robinson H, Goo YA, Goodlett DR, Raunser S, Mougous JD. 2015. An interbacterial
613 NAD(P)+ glycohydrolase toxin requires elongation factor Tu for delivery to target cells.
614 *Cell* 163:607–619.
- 615 26. Tang JY, Bullen NP, Ahmad S, Whitney JC. 2018. Diverse NADase effector families
616 mediate interbacterial antagonism via the type VI secretion system. *J Biol Chem*
617 293:1504–1514.
- 618 27. Ting S-YY, Bosch DE, Mangiameli SM, Radey MC, Huang S, Park Y-JJ, Kelly KA, Filip
619 SK, Goo YA, Eng JK, Allaire M, Veessler D, Wiggins PA, Peterson SB, Mougous JD.
620 2018. Bifunctional immunity proteins protect bacteria against FtsZ-targeting ADP-
621 Ribosylating toxins. *Cell* 175:1380-1392.e14.
- 622 28. Jurėnas D, Payelleville A, Roghanian M, Turnbull KJ, Givaudan A, Brillard J, Hauryliuk V,
623 Cascales E. 2021. Photorhabdus antibacterial Rhs polymorphic toxin inhibits translation
624 through ADP-ribosylation of 23S ribosomal RNA. *Nucleic Acids Res* 49.
- 625 29. Nolan LM, Cain AK, Clamens T, Furniss RCD, Manoli E, Sainz-Polo MA, Dougan G,
626 Albesa-Jové D, Parkhill J, Mavridou DAI, Filloux A. 2021. Identification of Tse8 as a type
627 VI secretion system toxin from *Pseudomonas aeruginosa* that targets the bacterial
628 transamidosome to inhibit protein synthesis in prey cells. *Nat Microbiol* 6.
- 629 30. de Moraes MH, Hsu F, Huang D, Bosch DE, Zeng J, Radey MC, Simon N, Ledvina HE,
630 Frick JP, Wiggins PA, Peterson SB, Mougous JD. 2021. An interbacterial dna deaminase
631 toxin directly mutagenizes surviving target populations. *Elife* 10.
- 632 31. Ahmad S, Wang B, Walker MD, Tran HKR, Stogios PJ, Savchenko A, Grant RA,
633 McArthur AG, Laub MT, Whitney JC. 2019. An interbacterial toxin inhibits target cell
634 growth by synthesizing (p)ppApp. *Nature* 575.
- 635 32. Ruhe ZC, Low DA, Hayes CS. 2020. Polymorphic toxins and their immunity proteins:
636 Diversity, evolution, and mechanisms of delivery. *Annu Rev Microbiol* 74:497–520.
- 637 33. Lien YW, Lai EM. 2017. Type VI secretion effectors: Methodologies and biology. *Front*
638 *Cell Infect Microbiol* <https://doi.org/10.3389/fcimb.2017.00254>.
- 639 34. Liang X, Moore R, Wilton M, Wong MJQ, Lam L, Dong TG. 2015. Identification of
640 divergent type VI secretion effectors using a conserved chaperone domain. *Proc Natl*
641 *Acad Sci* 112:9106–9111.
- 642 35. Dong TG, Ho BT, Yoder-Himes DR, Mekalanos JJ. 2013. Identification of T6SS-
643 dependent effector and immunity proteins by Tn-seq in *Vibrio cholerae*. *Proc Natl Acad*
644 *Sci* 110:2623–2628.
- 645 36. Salomon D, Kinch LN, Trudgian DC, Guo X, Klimko JA, Grishin N V., Mirzaei H, Orth K.
646 2014. Marker for type VI secretion system effectors. *Proc Natl Acad Sci* 111:9271–9276.
- 647 37. Dar Y, Jana B, Bosis E, Salomon D. 2021. A binary effector module secreted by a type VI

- 648 secretion system. EMBO Rep e53981.
- 649 38. Liang X, Pei TT, Li H, Zheng HY, Luo H, Cui Y, Tang MX, Zhao YJ, Xu P, Dong T. 2021.
650 VgrG-dependent effectors and chaperones modulate the assembly of the type VI
651 secretion system. PLoS Pathog 17:e1010116.
- 652 39. Manera K, Kamal F, Burkinshaw B, Dong TG. 2021. Essential functions of chaperones
653 and adaptors of protein secretion systems in Gram-negative bacteria. FEBS J
654 <https://doi.org/10.1111/FEBS.16056>.
- 655 40. Baker-Austin C, Oliver JD, Alam M, Ali A, Waldor MK, Qadri F, Martinez-Urtaza J. 2018.
656 *Vibrio* spp. infections. Nat Rev Dis Prim 4:1–19.
- 657 41. Yu Y, Yang H, Li J, Zhang P, Wu B, Zhu B, Zhang Y, Fang W. 2012. Putative type VI
658 secretion systems of *Vibrio parahaemolyticus* contribute to adhesion to cultured cell
659 monolayers. Arch Microbiol 194:827–835.
- 660 42. Li P, Kinch LN, Ray A, Dalia AB, Cong Q, Nunan LM, Camilli A, Grishin N V, Salomon D,
661 Orth K. 2017. Acute hepatopancreatic necrosis disease-causing *Vibrio parahaemolyticus*
662 strains maintain an antibacterial type VI secretion system with versatile effector
663 repertoires. Appl Environ Microbiol 83:e00737-17.
- 664 43. Salomon D, Gonzalez H, Updegraff BL, Orth K. 2013. *Vibrio parahaemolyticus* Type VI
665 secretion system 1 is activated in marine conditions to target bacteria, and is differentially
666 regulated from system 2. PLoS One 8:e61086.
- 667 44. Metzger LC, Matthey N, Stoudmann C, Collas EJ, Blokesch M. 2019. Ecological
668 implications of gene regulation by TfoX and TfoY among diverse *Vibrio* species. Environ
669 Microbiol 21:2231–2247.
- 670 45. Dar Y, Salomon D, Bosis E. 2018. The antibacterial and anti-eukaryotic Type VI secretion
671 system MIX-effector repertoire in Vibrionaceae. Mar Drugs 16:433.
- 672 46. Le Roux F, Blokesch M. 2018. Eco-evolutionary dynamics linked to horizontal gene
673 transfer in vibrios. Annu Rev Microbiol 72:annurev-micro-090817-062148.
- 674 47. Sun Y, Bernardy EE, Hammer BK, Miyashiro T. 2013. Competence and natural
675 transformation in vibrios. Mol Microbiol 89.
- 676 48. Salomon D, Klimko JA, Trudgian DC, Kinch LN, Grishin N V., Mirzaei H, Orth K. 2015.
677 Type VI secretion system toxins horizontally shared between marine bacteria. PLoS
678 Pathog 11:1–20.
- 679 49. Thomas J, Watve SS, Ratcliff WC, Hammer BK. 2017. Horizontal gene transfer of
680 functional type VI killing genes by natural transformation. MBio 8:1–11.
- 681 50. Ray A, Schwartz N, Souza Santos M, Zhang J, Orth K, Salomon D, de Souza Santos M,
682 Zhang J, Orth K, Salomon D. 2017. Type VI secretion system MIX-effectors carry both
683 antibacterial and anti-eukaryotic activities. EMBO Rep 18:e201744226.
- 684 51. Unterweger D, Kostiuk B, Pukatzki S. 2017. Adaptor proteins of type VI secretion system
685 effectors. Trends Microbiol 25:8–10.
- 686 52. Käll L, Krogh A, Sonnhammer EL. 2004. A combined transmembrane topology and signal
687 peptide prediction method. J Mol Biol 338:1027–1036.
- 688 53. Zhang D, de Souza RF, Anantharaman V, Iyer LM, Aravind L. 2012. Polymorphic toxin
689 systems: Comprehensive characterization of trafficking modes, processing, mechanisms
690 of action, immunity and ecology using comparative genomics. Biol Direct 7:18.

- 691 54. Lopez J, Le N-H, Moon KH, Salomon D, Bosis E, Feldman MF. 2021. Formylglycine-
692 generating enzyme-like proteins constitute a novel family of widespread type VI secretion
693 system immunity proteins. *J Bacteriol* 203.
- 694 55. Jana B, Keppel K, Salomon D. 2021. Engineering a customizable antibacterial T6SS-
695 based platform in *Vibrio natriegens*. *EMBO Rep* 22:e53681.
- 696 56. Salomon D, Klimko JA, Orth K. 2014. H-NS regulates the *Vibrio parahaemolyticus* type VI
697 secretion system 1. *Microbiol (United Kingdom)* 160:1867–1873.
- 698 57. Russell AB, Hood RD, Bui NK, Leroux M, Vollmer W, Mougous JD. 2011. Type VI
699 secretion delivers bacteriolytic effectors to target cells. *Nature* 475:343–349.
- 700 58. Ringel PD, Hu D, Basler M. 2017. The role of type VI secretion system effectors in target
701 cell lysis and subsequent horizontal gene transfer. *Cell Rep* 21:3927–3940.
- 702 59. Hersch SJ, Watanabe N, Stietz MS, Manera K, Kamal F, Burkinshaw B, Lam L, Pun A, Li
703 M, Savchenko A, Dong TG. 2020. Envelope stress responses defend against type six
704 secretion system attacks independently of immunity proteins. *Nat Microbiol* 5:706–714.
- 705 60. Hersch SJ, Manera K, Dong TG. 2020. Defending against the Type Six Secretion
706 System: beyond Immunity Genes. *Cell Rep* 33:108259.
- 707 61. Aoki SK, Diner EJ, de Roodenbeke C t'Kint, Burgess BR, Poole SJ, Braaten BA, Jones
708 AM, Webb JS, Hayes CS, Cotter PA, Low DA. 2010. A widespread family of polymorphic
709 contact-dependent toxin delivery systems in bacteria. *Nature* 468:439–442.
- 710 62. Tran L, Nunan L, Redman R, Mohny L, Pantoja C, Fitzsimmons K, Lightner D. 2013.
711 Determination of the infectious nature of the agent of acute hepatopancreatic necrosis
712 syndrome affecting penaeid shrimp. *Dis Aquat Organ* 105:45–55.
- 713 63. Borgeaud S, Metzger LC, Scignari T, Blokesch M. 2015. The type VI secretion system of
714 *Vibrio cholerae* fosters horizontal gene transfer. *Science* 347:63–7.
- 715 64. Matthey N, Stutzmann S, Stoudmann C, Guex N, Iseli C, Blokesch M. 2019. Neighbor
716 predation linked to natural competence fosters the transfer of large genomic regions in
717 *vibrio cholerae*. *Elife* 8.
- 718 65. Gibson DG, Young L, Chuang RY, Venter JC, Hutchison CA, Smith HO. 2009. Enzymatic
719 assembly of DNA molecules up to several hundred kilobases. *Nat Methods* 6:343–345.
- 720 66. O'Toole R, Milton DL, Wolf-Watz H. 1996. Chemotactic motility is required for invasion of
721 the host by the fish pathogen *Vibrio anguillarum*. *Mol Microbiol* 19:625–637.
- 722 67. Lee I, Ouk Kim Y, Park S-C, Chun J. 2016. OrthoANI: An improved algorithm and
723 software for calculating average nucleotide identity. *Int J Syst Evol Microbiol* 66:1100–
724 1103.
- 725 68. Camacho C, Coulouris G, Avagyan V, Ma N, Papadopoulos J, Bealer K, Madden TL.
726 2009. BLAST+: Architecture and applications. *BMC Bioinformatics* 10.
- 727 69. Altschul SF, Madden TL, Schäffer AA, Zhang J, Zhang Z, Miller W, Lipman DJ. 1997.
728 Gapped BLAST and PSI-BLAST: a new generation of protein database search programs.
729 *Nucleic Acids Res* 25:3389–402.
- 730 70. Marchler-Bauer A, Bo Y, Han L, He J, Lanczycki CJ, Lu S, Chitsaz F, Derbyshire MK,
731 Geer RC, Gonzales NR, Gwadz M, Hurwitz DI, Lu F, Marchler GH, Song JS, Thanki N,
732 Wang Z, Yamashita RA, Zhang D, Zheng C, Geer LY, Bryant SH. 2017. CDD/SPARCLE:
733 functional classification of proteins via subfamily domain architectures. *Nucleic Acids Res*

- 734 45:D200–D203.
- 735 71. Katoh K, Misawa K, Kuma K, Miyata T. 2002. MAFFT: a novel method for rapid multiple
736 sequence alignment based on fast Fourier transform. *Nucleic Acids Res* 30:3059–66.
- 737 72. Katoh K, Rozewicki J, Yamada KD. 2018. MAFFT online service: Multiple sequence
738 alignment, interactive sequence choice and visualization. *Brief Bioinform* 20:1160–1166.
- 739 73. Saitou N, Nei M. 1987. The neighbor-joining method: a new method for reconstructing
740 phylogenetic trees. *Mol Biol Evol* 4:406–425.
- 741 74. Sievers F, Wilm A, Dineen D, Gibson TJ, Karplus K, Li W, Lopez R, McWilliam H,
742 Remmert M, Söding J, Thompson JD, Higgins DG. 2011. Fast, scalable generation of
743 high-quality protein multiple sequence alignments using Clustal Omega. *Mol Syst Biol*
744 7:539.
- 745 75. Kumar S, Stecher G, Li M, Knyaz C, Tamura K. 2018. MEGA X: Molecular evolutionary
746 genetics analysis across computing platforms. *Mol Biol Evol* 35:1547–1549.
- 747 76. Marchler-Bauer A, Anderson JB, Derbyshire MK, DeWeese-Scott C, Gonzales NR,
748 Gwadz M, Hao L, He S, Hurwitz DI, Jackson JD, Ke Z, Krylov D, Lanczycki CJ, Liebert
749 CA, Liu C, Lu F, Lu S, Marchler GH, Mullokandov M, Song JS, Thanki N, Yamashita RA,
750 Yin JJ, Zhang D, Bryant SH. 2007. CDD: a conserved domain database for interactive
751 domain family analysis. *Nucleic Acids Res* 35:D237-40.
- 752 77. Zimmermann L, Stephens A, Nam S-Z, Rau D, Kübler J, Lozajic M, Gabler F, Söding J,
753 Lupas AN, Alva V. 2018. A completely reimplemented MPI bioinformatics toolkit with a
754 new HHpred server at its core. *J Mol Biol* 430:2237–2243.
- 755